J Appl Physiol 106: 1686–1691, 2009.
First published March 19, 2009; doi:10.1152/japplphysiol.91519.2008.

TRANSLATIONAL PHYSIOLOGY

Effects of stent sizing on endothelial and vessel wall stress: potential mechanisms for in-stent restenosis

Henry Y. Chen,[1,6] James Hermiller,[2] Anjan K. Sinha,[3] Michael Sturek,[5,6] Luoding Zhu,[4] and Ghassan S. Kassab[1,5,6,7]

[1]*Weldon School of Biomedical Engineering, Purdue University, West Lafayette;* [2]*Department of Cardiovascular Surgery, St. Vincent Hospital, Indianapolis; and Departments of* [3]*Medicine (Cardiology),* [4]*Mathematical Sciences,* [5]*Surgery,* [6]*Cellular and Integrative Physiology, and* [7]*Biomedical Engineering, Indiana University Purdue University Indianapolis, Indianapolis, Indiana*

Submitted 21 November 2008; accepted in final form 13 March 2009

Chen HY, Hermiller J, Sinha AK, Sturek M, Zhu L, Kassab GS. Effects of intravascular stent sizing on endothelial and vessel wall stress: potential mechanisms of in-stent restenosis. *J Appl Physiol* 106: 1686–1691, 2009. First published March 19, 2009; doi:10.1152/japplphysiol.91519.2008.—Stent sizing and apposition have been shown to be important determinants of clinical outcome. This study evaluates the mechanical effects of undersizing and oversizing of stents on endothelial wall shear stress (WSS) and vessel wall stress to determine a possible biomechanical mechanism of in-stent restenosis and thrombosis. Three-dimensional computational models of stents, artery, and internal fluid were created in a computer-assisted design package, meshed, and solved in finite element and computational fluid dynamic packages. The simulation results show that the effects of various degrees of undersizing on WSS, WSS gradient, and oscillatory shear index were highly nonlinear. As the degree of undersizing increased, the heterogeneity of WSS became smaller. The WSS distribution for the 20% undersizing was smooth and uniform, whereas the 5% case was very heterogeneous. The combination of lower WSS and higher WSS gradient and oscillatory shear index in the 5% undersized case may induce neointimal hyperplasia or thrombosis. Additionally, the oversizing simulation results show that the maximum intramural wall stress of the 20% oversizing case is significantly larger than the maximum stress for the 10% and zero oversizing cases. Edge stress concentration was observed, consistent with the restenosis typically observed in this region. This study demonstrates that proper sizing of stent is important for reducing the hemodynamic and mechanical disturbances to the vessel wall. Furthermore, the present findings may be used to improve stent design to reduce endothelial flow disturbances and intramural wall stress concentrations.

undersizing; oversizing; intimial hyperplasia; shear stress

FOR OVER TWO DECADES, VASCULAR stents have been used to treat vessel stenosis, serving as a scaffold for arterial patency. In some cases, however, neointimal hyperplasia after stenting leads to in-stent restenosis (ISR) (8). Because of their ability to substantially attenuate neointimal formation following stenting, drug eluted stents (DES) were projected to largely eliminate the restenosis problem. Restenosis with DES is significant (22, 30), however, and there is increased risk of late thrombosis (1, 31), particularly in complex lesion subsets. Finally, DES does not address the fundamental fluid (flow disturbances) and solid mechanics (compliance mismatch) associated with stents, which can significantly contribute to ISR.

Experimental and clinical evidence suggests that alteration of wall shear stress (WSS) contributes to the occurrence of ISR. Specifically, it has been observed clinically that the sites of ISR or neointima hyperplasia highly correlate with sites of low WSS (27). Furthermore, nonuniform WSS was also found to contribute to cell migration and differentiation after stent implantation. During stent deployment, the intima and media may be injured acutely, and the struts compress the vessel wall chronically. These stress concentrations and associated injuries are very likely to provoke inflammatory responses that may initiate atherogenesis (4, 5).

Analysis of stent designs and their associated fluid and solid stress patterns can lead to better stent deployment to minimize hyperplasia and restenosis and to improve stent designs. Here, we hypothesize that stent undersizing leads to disturbed flows and low WSS near the struts while stent oversizing leads to high intramural wall stress especially at the stent edges. The present study validates these hypotheses and postulates the potential clinical implications of these findings.

METHODS

A three-dimensional (3D) computational model of a stent, artery, and blood was created in Pro/Engineer, which is a Computer-Assisted Design package (Fig. 1). The models were then interfaced, meshed, and solved in well-validated finite element and computational fluid dynamic packages ANSYS and FLOTRAN. The geometry of stent was modeled as the typical diamond-shaped slotted tube design (12 mm long with 0.25-mm strut thickness). The vessel wall thickness was 0.8 mm. A 10 and 20% oversized stent models and 5, 10, and 20% undersized stent models (diameters sized relative to vessel diameter of 3 mm) were created for the simulations.

Governing equations. The governing equations for the fluid domain were the Navier-stokes and Continuity equations (9):

$$\frac{\partial \vec{V}}{\partial t} + \vec{V}\cdot\vec{\nabla}\vec{V} + \frac{\vec{\nabla}p}{\rho} - 2\frac{\eta}{\rho}\vec{\nabla}\cdot D = \vec{0} \quad (1)$$

$$\vec{\nabla}\cdot\vec{V} = 0 \quad (2)$$

where V is velocity, p is pressure, ρ is density, η is viscosity, $\vec{\nabla}$ is the gradient operator, and D is the rate of deformation tensor.

The governing equations for the solid domain were the Momentum and Equilibrium equations (12):

Address for reprint requests and other correspondence: G. S. Kassab, Indiana Univ. Purdue Univ. Indianapolis, Biomedical Engineering, SL-174, 723 West Michigan St., Indianapolis, Indiana 46202.

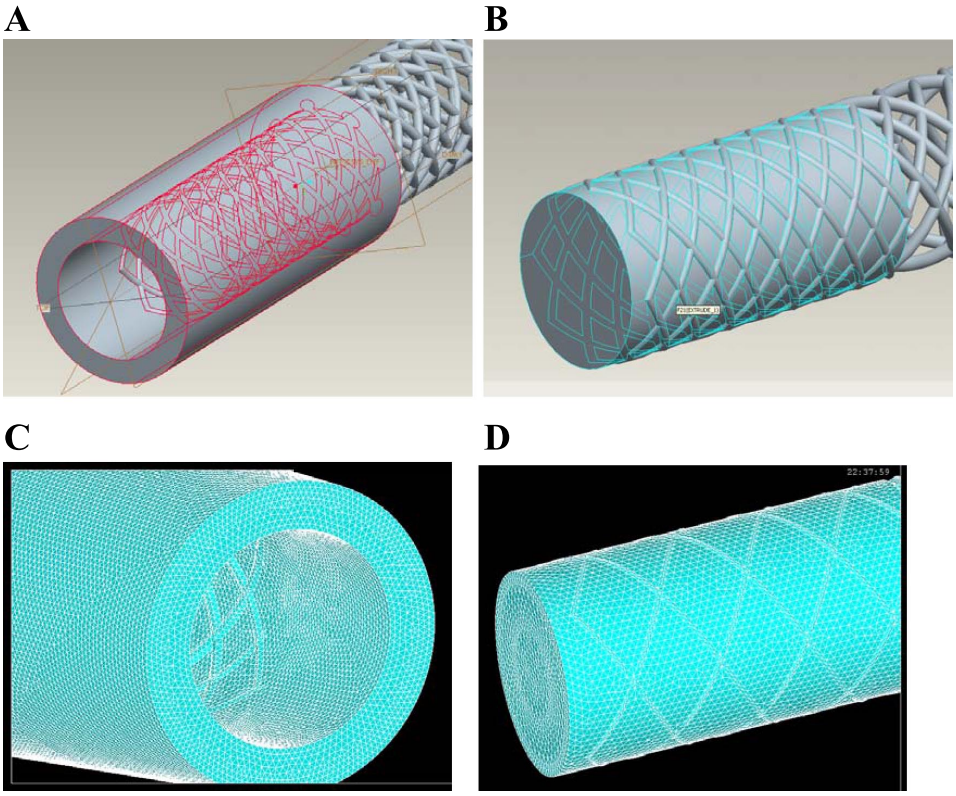

Fig. 1. *A*: geometries of the solid components: stent and vessel. *B*: geometry of blood with the stent shown. *C*: highly structured and refined meshes of the solid components: a stent within an artery. *D*: meshes of the fluid with the strut pattern shown.

$$\rho a_i - \sigma_{ij,j} - \rho f_i = 0 \quad \text{in} \quad {}^s\Omega(t) \tag{3}$$

$$\sigma_{ij} n_j - t_i = 0 \quad \text{on} \quad {}^s\Gamma(t) \tag{4}$$

where a_i is acceleration of a material point, f_i is force per unit mass, ${}^s\Omega(t)$ is the structural domain at time t, t_i is surface traction vector, σ_{ij} is stress; n_j is outward normal vector, and ${}^s\Gamma(t)$ is the boundary. The mathematical formulations for additional fluid and solid components and outputs were described in detail in the APPENDIX.

The meshes of the stent and artery consisted of highly structured and refined elements to ensure the accuracy of simulation results. About 1.2 million mesh elements were used in the simulations. A mesh convergence test showed that doubling the number of elements only resulted in <3% difference in WSS, WSSG, and peak von Mises stresses. The stress distributions also did not change appreciably. Hence, the mesh density was sufficient for the proposed simulations.

To model the bending motion of the coronary arteries, a typical 30° bending was prescribed on the artery wall, similar to that used by Stein et al. (28). The density and viscosity of the blood were taken as 1,060 kg/m^3 and 0.004 kg·m^{-1}·s^{-1} respectively. The blood was modeled as incompressible with flow based on human coronary artery velocity measurements, applied at the inlet of vessel (14). For the outlet of the vessels, a zero-traction boundary condition was imposed (16). At the wall interface, we assume no slip between blood and the endothelium and no permeability of the vessel wall.

RESULTS

The simulation results were independent of the time steps, as various time steps were attempted and the resulting WSS, WSSG patterns, and magnitudes were very similar. A total of 140 time steps were used for the study. The simulations ran for an average of 20 h.

For blood flow, the WSS distribution for different undersized stent simulations is shown in Figs. 2–4. Although these figures appear two-dimensional, they are side views of the 3D models. As shown in the geometry and mesh in Fig. 1, these models are fully 3D. As the extent of undersizing increases, the spatial heterogeneity (quantified by the coefficient of variance = SD/mean) of WSS becomes smaller. In the 20% case, there is little difference between the high and low end range of WSS, which suggests a small spatial WSS gradient (WSSG). As shown in Figs. 2–4, the WSS distribution for the 20% case is homogenous, whereas the 5% case shows significant heterogeneity.

Figures 2–4 alsoshow the WSS and WSSG profile in the 5, 10, and 20% undersized cases, respectively. The presence of stent struts decreases the WSS, but increases the WSSG. This effect is less significant in the 20% undersized case. The proximal edge promotes lower WSS than the distal edge, and both edges reflect higher WSSG than the middle portion of stented vessel. Figures 2–4 show that the stent lowers the WSS (compared with the no-stent case), but increases the WSSG near the struts. Compared with the 5% undersized case, the correct sized case produced higher WSS, lower WSSG, and lower oscillatory shear index (OSI). The plots in Fig. 5 show that the effects of degrees of undersizing on the WSS, WSSG, and OSI are highly nonlinear. These values are for the lowest WSS, highest WSSG, and OSI along the stented vessel wall, as they are known to promote intimal hyperplasia.

For the stent oversizing, Fig. 6*A* shows the von Mises (overall effective) stress distribution (N/cm^2, equivalent to 10 kPa) in the case of 10% oversizing. The von Mises stress combines the 3D components of mechanical stresses and reflects the overall effective stress. Stress concentrations are observed around the edges of stent, which are consistent with restenosis typically observed in this region. Figure 6*B* shows that the maximum stress for the 20% oversizing (112 N/cm^2) is

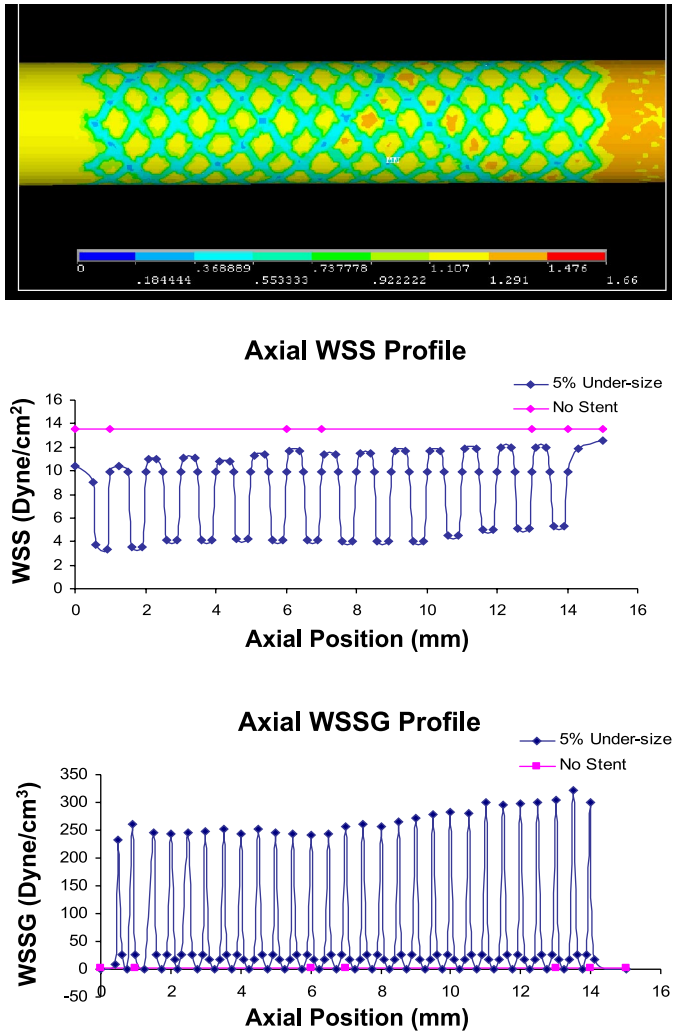

Fig. 2. *Top*: wall shear stress (WSS) distribution (Pa) with 5% undersized stent [frontal view of three-dimensional (3D) model]. The proximal region has lower WSS than the distal region. *Middle*: the WSS. *Bottom*: WSS gradient (WSSG) profile in the 5% undersized case. The presence of struts lowers the WSS and elevates the WSSG.

significantly larger than the maximum stress for the 10% oversizing case (68 N/cm^2) and much larger than for the zero oversizing case (37 N/cm^2).

DISCUSSION

The major finding of this study is that the degree of undersizing significantly affects WSS, WSSG, and OSI, which may promote intimal hyperplasia, thrombosis, and atherogenesis. Conversely, oversizing significantly increases the intramural stress, which can acutely cause vessel dissection or chronically stimulate smooth muscle proliferation and initiate an inflammatory response. These fluid/solid biomechanics simulations of vessel/stent underscore the significance of proper stent sizing. Specifically, the present study evaluated the axial WSS, WSSG, and the solid wall stress profiles of a stented vessel. It was found that low WSS exists near the struts, especially at the proximal end. Higher wall stress concentrations were present at the stent edges. This correlates with the edge restenosis observed clinically at the stent edges, especially at the proximal end.

Undersizing of stent. There is a tendency toward undersizing, as oversizing deployments can lead to accurate events, such as dissections, during interventions. Although undersizing may not affect the immediate outcome of the stenting procedures, the present study demonstrates that such undersizing significantly lowers WSS near the struts. This may contribute to thrombosis and hyperplasia in the longer term. Late stent thrombosis has been found to be an increasingly significant problem for DES in recent years, and undersizing has been considered an important culprit (1, 31).

The effects of degrees of undersizing on WSS, WSSG, and OSI were found to be nonlinear. Furthermore, as the extent of undersizing increases, the spatial heterogeneity of WSS becomes smaller. In the 20% case, there is little heterogeneity of WSSG. The 5% case reflects the converse, and both the low WSS and high spatial WSSG may contribute to intimal hyperplasia. The presence of undersized stent lowers the WSS, but increases the WSSG significantly near the struts. The low-WSS pattern corresponding to the struts pattern may induce throm-

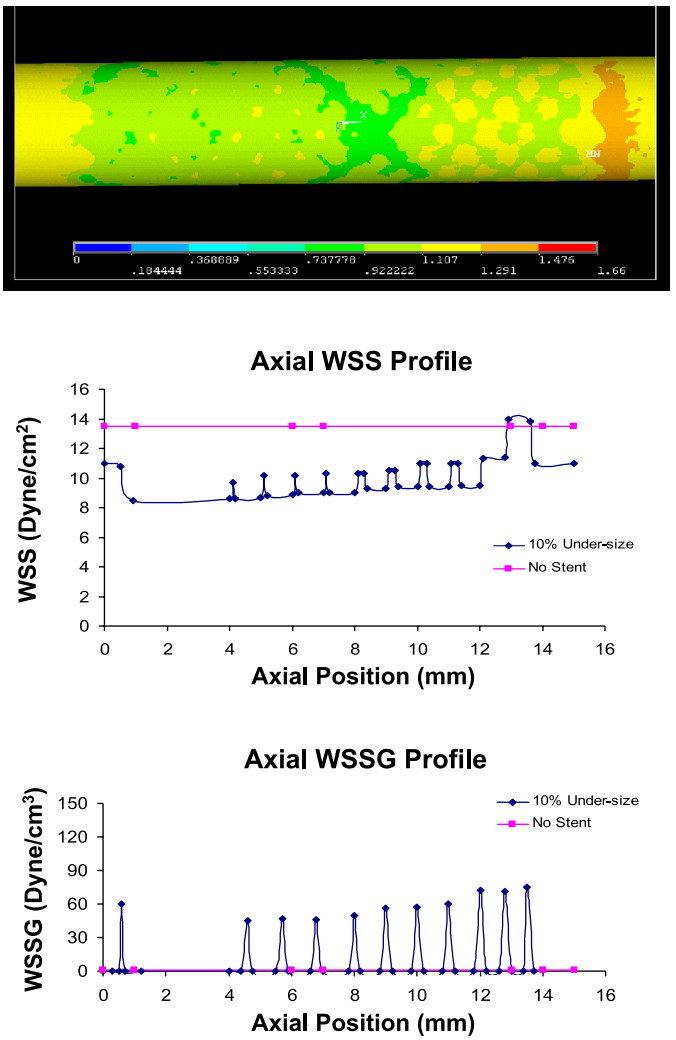

Fig. 3. *Top*: WSS distribution (Pa) with 10% undersized stent (frontal view of 3D model). The proximal entrance region has lower WSS than the distal region. *Middle*: the WSS. *Bottom*: WSSG profile in the 10% undersized case. The presence of stent struts lowers the WSS, while elevating the WSSG compared with the no-stent case.

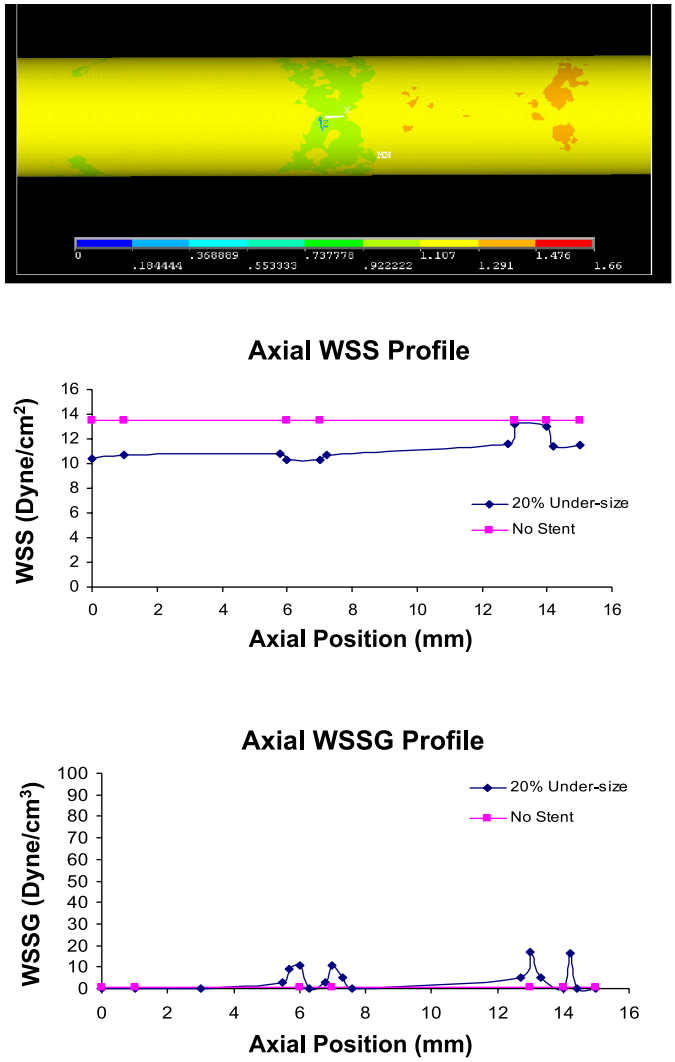

Fig. 4. *Top*: WSS distribution (Pa) with 20% undersized stent (frontal view of 3D model). The proximal entrance region has lower WSS than the distal region. *Middle*: the WSS. *Bottom*: WSSG profile in the 20% undersized case. The WSS distribution is nearly uniform, leading to the lower WSSG. The no-stent case is also shown for comparison.

bosis. Low fluid shear stress can cause red blood cells to adhere to each other, which may initiate the clotting cascade. Liu et al. (17) found that an initiator of the coagulation cascade, tissue factor, was upregulated by low shear stress. Tissue factor catalyzes the conversion of prothrombin to thrombin. In addition, WSSG has been found to contribute to cell migration and differentiation after stent implantation (17).

The WSS is highly dependent on the near-wall condition. It should be noted that, in the case of 5% undersizing, the tiny gaps between the stent struts and wall increase the local flow resistance near the wall and create low shear regions. Compared with the correct-sized (0%) case, the WSS is significantly lower, while WSSG and OSI are significantly higher. This effect becomes less pronounced as the stent is further away from the wall in the 10 and 20% undersized cases. As the distances between the struts and wall become larger, the local flow resistance is decreased, and the low shear regions diminish (Figs. 2–4).

Oversizing of stent. There is a tendency to oversize stents by 10% to ensure stent apposition. Since sizing is typically approximated, larger oversizing (20%) can significantly increase the vessel wall stress and may induce inflammatory response, which, in turn, contributes to neointimal hyperplasia. Additionally, the coronary arteries are unique compared with most other vessels, in that they undergo significant bending motion due to the heart contractions. The bending or flexion was found to additionally influence coronary wall stress (26).

Oversizing was found to significantly increase the intramural wall stress. The overall von Mises stress in the 20% oversizing case was significantly higher than the 10% oversizing and the zero oversizing cases, which may cause vascular injury (7). This is especially manifested at the stent edge regions. The high prevalence of neointimal hyperplasia at stent/artery transition regions is known as the edge effect.

Mechanical stresses and vessel function. Besides the well-known effects of fluid shear stresses on the endothelium (10, 15, 19, 20, 21, 25), the solid stresses within the wall (including media) may also play an important role in vessel injury and remodeling (18). It is known that altered stress states in tissue (i.e., hypertension) can stimulate remodeling and cellular proliferation (6, 11, 23, 24, 28). The stent struts cause stress concentrations, which may lead to inflammation and vessel injury. Furthermore, the low WSS patterns caused by the struts are likely to induce thrombosis, as discussed earlier. The thrombosis associated with stent deployment may also provide a scaffold for neointima hyperplasia (17), and the platelets may release platelet-derived growth factor that attracts inflammatory cells. The stent placement causes static stresses and strains, which may lead to cellular proliferation (7, 32). It is plausible that the stresses (fluid and solid) act in synergy. The endothelium senses the fluid shear stress, which initiates mechanotransduction and signal transduction to produce growth factors and enzymes, such as fibroblast growth factor (21, 29).

An important determinant of the vessel health after stent placement is the rate and extent of in-stent reendothelialization. This is due to the fact that the new endothelial layer prevents thrombosis by isolating the thrombogenic metallic stent struts and the underlying plaque from the circulating prothrombotic factors. A possible mechanism for circulating progenitor cell [endothelial progenitor cell (EPC)] deposition is that the stent deployment causes vessel wall injury, which may provoke inflammatory response and homing of the circulating EPCs to the injury site to deposit on the stent surface. This is analogous to smooth muscle precursor cells homing to the site of inflammation surrounding vascular plaques (2, 7). The EPC deposition may be related to WSS, as the rate of deposition of cells depends on WSS, which is the shear force acting on the wall surface. This is the force that cells directly experience as they deposit on the vessel surface. A lower WSS is more inducive to neointima hyperplasia. Thus the magnitude and patterns of WSS related to stent sizing are of critical importance.

Model limitations. The present model did not incorporate plaque morphology in the vessel wall. Future models can include the nonhomogenous structure of the vessel wall, including calcification and lipid pool. Furthermore, the current model assumes that the undersizing or oversizing occurs uniformly along the length of the stent. In reality, some portions of the stent may be well apposed, whereas others may not, along the plaque. Oversizing may occur at

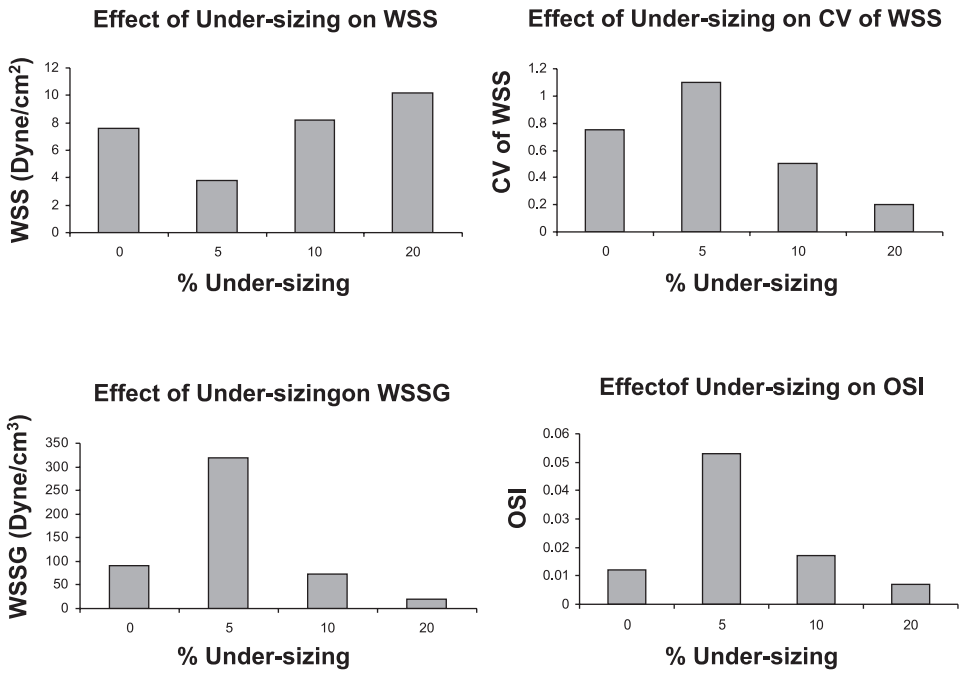

Fig. 5. The effects of degrees of undersizing on WSS, WSSG, oscillatory shear index (OSI) and coefficient of variance (CV = SD/mean) of WSS are nonlinear for the correct-sized (0%) and 5, 10, and 20% undersized cases.

the throat of the stenotic region, and undersizing is more likely in the expanded region outside the throat. Given the level of complexity of such models, it is necessary to take a step-by-step approach.

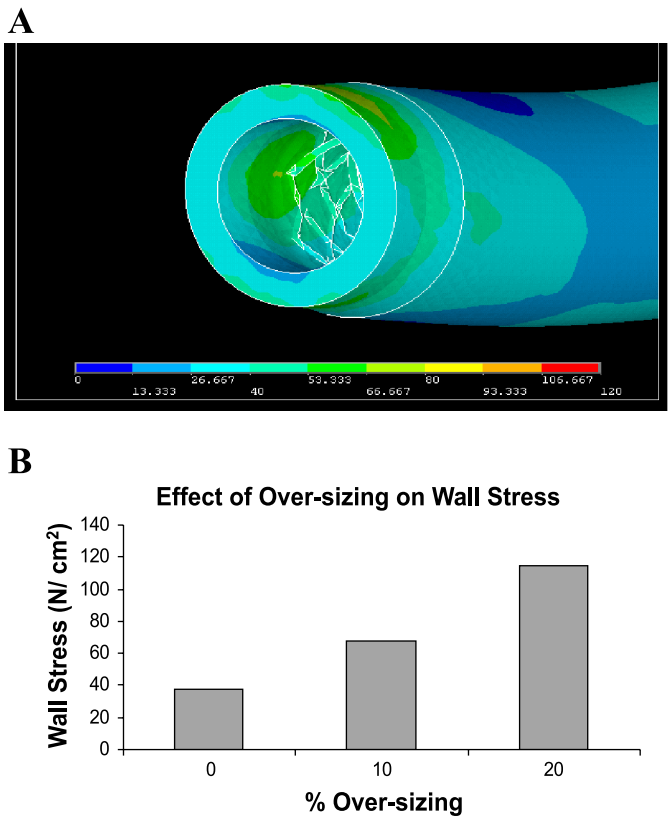

Fig. 6. *A*: von Mises wall stress distribution (N/cm^2 = 10 kPa) in the case of 10% oversizing. Stent edge stress concentration is demonstrated. *B*: the effects of degrees of oversizing on von Mises wall stresses.

The stent struts simulated in the present study have circular cross sections. Other commercial stents have more rectangular-shaped struts, which likely will increase the WSSG, as WSS changes more abruptly near the edges of struts, compared with smooth circular struts.

The models in the present study are created using Pro-Engineer. Pro-Engineer is a 3D CAD software that is based on parametric model construction. Design optimizations are possible using parametric software, such as Pro-Engineer and optimization software such as LS-OPT, Mathematica, and others. In the future, response surface (LS-OPT) and gradient based methods (Mathematica) may be used to optimize various stent designs.

The strut thickness modeled is relatively thick (250 μm) compared with some commercial stents with thicknesses in the range of 150 μm. In the simulations, especially the 5% undersized case, the low WSS areas corresponded to the diamond strut pattern. In this case, thinner struts may likely result in narrower bands of low WSS region. The WSS magnitudes, however, are not expected to change significantly. Additionally, arteries may be tortuous but become straight once the stent is implanted. Since the clinically observed restenosis mainly occurs within the stented region, a straight segment was simulated here.

Significance. The simulations of fluid and solid mechanics of stent sizing suggest potential mechanisms of ISR, thrombosis, or dissection. These numerical predictions provide a basis for future additional experiments to connect vessel biology and function to stent biomechanics. Furthermore, the present model may serve as a guide for improved stent designs. The detailed stress and fluid analysis cannot be easily measured experimentally. Mathematical models can be used for design optimization, i.e., to obtain the optimal pattern and thickness of struts, etc., that produce minimal flow and wall disturbances. These simulations may save both time and cost of building and testing various prototypes.

APPENDIX

WSSG and OSI formulations. The WSSG, which has been found to expand intracellular gap junctions and disrupt intracellular junctions, is defined as:

$$\mathrm{WSSG} = \left[\left(\frac{\partial \tau_{w,z}}{\partial z} \right)^2 + \left(\frac{\partial \tau_{w,\theta}}{\partial \theta} \right)^2 \right]^{1/2} \quad (A1)$$

where $\tau_{w,z}$ and $\tau_{w,\theta}$ are WSS in the axial and circumferential directions, respectively.

The OSI is a measure of the extent of oscillatory behavior of flow, which has been found to promote pathological processes in arteries. The time-averaged OSI is defined by Ku et al. (15) as:

$$\mathrm{OSI} = \frac{1}{2} \left(1 - \frac{\left| \frac{1}{T} \int_0^T \vec{\tau} \, \mathrm{d}t \right|}{\frac{1}{T} \int_0^T |\vec{\tau}| \mathrm{d}t} \right) \quad (A2)$$

where T is time of a cardiac cycle. Both WSSG and OSI were computed once the respective stress components were calculated from the computational fluid dynamics analysis.

Material model formulations. The artery was modeled as a soft and nonlinear material. The Strain Energy Function has the form:

$$\bar{\psi}(\bar{I}_1) = \frac{c}{2} (\bar{I}_1 - 3) \quad (A3)$$

where I_1 is the first invariant of the modified Cauchy-Green tensor; c is a material parameter with a value of 30 kPa (13). The parameter value was determined based on experimental data for human coronary arteries (3). For the stent material (stainless steel), the Young modulus is 200 GPa, and the Poisson ratio is 0.3.

ACKNOWLEDGMENTS

The first author appreciates the helpful discussions with Drs. Wei Zhang, Yi Liu, and Jose N. Navia at the Cleveland Clinic.

GRANTS

This research was supported in part by the National Heart, Lung, and Blood Institute Grants HL087235 and HL084529 (G. Kassab) and US National Science Foundation Grant DMS-0713718 (L. Zhu).

REFERENCES

1. **Camenzind E, Steg PG, Wijns W.** Stent thrombosis late after implantation of first-generation drug-eluting stents. *Circulation* 115: 1440–1455, 2007.
2. **Caplice NM.** Biologic alternatives to stents and grafts. *Curr Cardiol Rep* 3: 17–21, 2001.
3. **Carmines DV, McElhaney JH, Stack R.** A piece-wise nonlinear elastic stress expression of human and pig coronary arteries tested in vitro. *J Biomech* 24: 899–906, 1991.
4. **Davies PF.** Endothelial mechanisms of flow-mediated athero-protection and susceptibility. *Circ Res* 101: 10–12, 2007.
5. **Davies PF, Spaan JA, Krams R.** Shear stress biology of the endothelium. *Ann Biomed Eng* 33: 1714–1718, 2005.
6. **Deiwick M, Glasmacher B, Baba HA, Roeder N, Reul H, von Bally G, Scheld HH.** In vitro testing of bioprostheses: influence of mechanical stresses and lipids on calcification. *Ann Thorac Surg* 66, *Suppl* 6: S206–S211, 1998.
7. **Edwards JM, Alloosh MA, Long XL, Dick GM, Lloyd PG, Mokelke EA, Sturek M.** Adenosine A1 receptors in neointimal hyperplasia and in-stent stenosis in Ossabaw miniature swine. *Coron Artery Dis* 19: 27–31, 2008.
8. **Erbel R, aude M, Hopp HW, de Jaegere P, Serruys P, Rutsch W, Probst. P.** Coronary-artery stenting compared with balloon angioplasty for restenosis after initial balloon angioplasty. Restenosis stent study group. *N Engl J Med* 339: 1672–1678, 1998.
9. **Fefferman Charles L.** *Existence and Smoothness of the Navier-Stokes Equation*. Princeton, NJ: Department of Mathematics, Princeton University, 2000.
10. **Friedman MH, Bargeron CB, Deters OJ, Hutchins GM, Mark FF.** Correlation between wall shear and intimal thickness at a coronary artery branch. *Atherosclerosis* 68: 27–33, 1987.
11. **Fung YC.** *Biomechanics: Circulation*. New York: Springer-Verlag, 1996.
12. **Fung YC.** *Biomechanics: Motion, Flow, Stress, and Growth*. New York: Springer-Verlag, 1998.
13. **Gasser TC, Schulze-Bauer CA, Holzapfel GA.** A three-dimensional finite element model for arterial clamping. *J Biomech Eng* 124: 355–363, 2002.
14. **Jung JW, Lyczkowski RW, Panchal CB, Hassanein A.** Multiphase hemodynamic simulation of pulsatile flow in a coronary artery. *J Biomech* 39: 2064–2073, 2006.
15. **Ku DN, Giddens DP, Zarins CK, Glagov S.** Pulsatile flow and atherosclerosis in the human carotid bifurcation. Positive correlation between plaque location and low oscillating shear stress. *Arteriosclerosis* 5: 293–302, 1985.
16. **LaDisa JF Jr, Olson LE, Hettrick DA, Warltier DC, Kersten JR, Pagel PS.** Axial stent strut angle influences wall shear stress after stent implantation: analysis using 3D computational fluid dynamics models of stent foreshortening. *Biomed Eng Online* 4: 59, 2005.
17. **Liu SQ, Zhong L, Goldman J.** Control of the shape of a thrombus, neointima-like structure by blood shear stress. *J Biomech Eng* 124: 30–36, 2002.
18. **Lu X, Kassab GS.** Nitric oxide is significantly reduced in ex vivo porcine arteries during reverse flow because of increased superoxide production. *J Physiol* 561: 575–582, 2004.
19. **Malek AM, Alper SL, Izumo S.** Hemodynamic shear stress and its role in atherosclerosis. *JAMA* 282: 2035–2042, 1999.
20. **Moore JE Jr, Xu C, Glagov S, Zarins CK, Ku DN.** Fluid wall shear stress measurements in a model of the human abdominal aorta: oscillatory behavior and relationship to atherosclerosis. *Atherosclerosis* 110: 225–240, 1994.
21. **Pavalko FM, Norvell SM, Burr DB, Turner CH, Duncan RL, Bidwell JP.** A model for mechanotransduction in bone cells: the load-bearing mechanosomes. *J Cell Biochem* 88: 104–112, 2003.
22. **Rogers C, Edelman ER.** Pushing drug-eluting stents into uncharted territory: simpler than you think–more complex than you imagine. *Circulation* 113: 2262–2265, 2006.
23. **Salzar RS, Thubrikar MJ, Eppink RT.** Pressure-induced mechanical stress in the carotid artery bifurcation: a possible correlation to atherosclerosis. *J Biomech* 28: 1333–1340, 1995.
24. **Schoen FJ, Levy RJ.** Calcification of tissue heart valve substitutes: progress toward understanding and prevention. *Ann Thorac Surg* 79: 1072–1080, 2005.
25. **Seo T, Schachter LG, Barakat AI.** Computational study of fluid mechanical disturbance induced by endovascular stents. *Ann Biomed Eng* 33: 444–456, 2005.
26. **Stein PD, Hamid MS, Shivkumar K, Davis TP, Khaja F, Henry JW.** Effects of cyclic flexion of coronary arteries on progression of atherosclerosis. *Am J Cardiol* 73: 431–437, 1994.
27. **Stone PH, Coskun AU, Kinlay S, Clark ME, Sonka M, WahleA, Ilegbusi OJ, Yeghiazarians Y, Popma JJ, Orav J, Kuntz RE, Feldman CL.** Effect of endothelial shear stress on the progression of coronary artery disease, vascular remodeling, and in-stent restenosis in humans: in vivo 6-month follow up study. *Circulation* 108: 438–444, 2003.
28. **Thubrikar MJ, Baker JW, Nolan SP.** Inhibition of atherosclerosis associated with reduction of arterial intramural stress in rabbits. *Arteriosclerosis* 8: 410–420, 1988.
29. **Turner CH, Pavalko FM.** Mechanotransduction of the skeleton to physical stress: the mechanisms and mechanics of bone adaptation. *J Orthop Sci* 3: 346–355, 1998.
30. **Virmani R, Farb A, Guagliumi G, Kolodgie FD.** Drug-eluting stents: caution and concerns for long-term outcome. *Coron Artery Dis* 15: 313–318, 2004.
31. **Wernick MH, Jeremias A, Carrozza JP.** Drug-eluting stents and stent thrombosis. *Coron Artery Dis* 17: 661–665, 2006.
32. **White CR, Haidekker M, Bao X, Frangos JA.** Temporal gradients in shear, but not spatial gradients, stimulate endothelial cell proliferation. *Circulation* 103: 2508–2513, 2001.